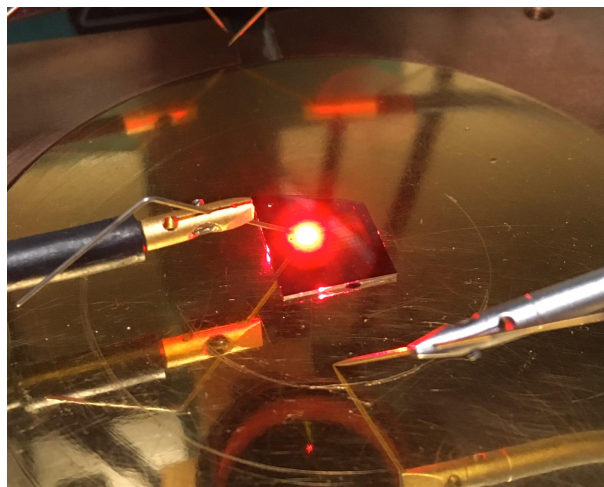


# ENG5055: Micro and Nano Technology: Manufacture of a Red LED

Angus Bruce - 2186197b

Tuesday 7<sup>th</sup> April, 2020



James Watt School of Engineering  
University of Glasgow

# 1 Introduction

An LED emit photons due to the recombination of electrons and holes when a potential difference is applied across it. LEDs are almost always made from a direct bandgap semiconductor such as GaAs as the recombination rate is higher due to the probability of a phonon, electron and hole being in close proximity is lower in an indirect bandgap semiconductor such as silicon. The wavelength of light produced by an LED depends largely on its bandgap. Using InGaAsP and altering the ratios, the bandgap can be tailored. Using InGaAsP and other direct bandgap semiconductors, LEDs are able to produce a wide range of wavelengths ranging from infrared through visible to ultraviolet.

The applications of LEDs in the world today are as useful as they are varied. In the home, LEDs provide energy-efficient long-lifetime lighting, far outperforming traditional incandescent bulbs. Due to their high ratio of optical power to area, it is possible to make high-resolution displays and screens from them. They are used in streetlights, reducing their running cost and carbon footprints. Small LEDs can be switched on an off very quickly making them suitable for using in optical communication systems. Since it is possible to engineer LEDs with tight wavelengths, LEDs can be useful in wavelength division multiplexing which can vastly increase the bandwidth of a given channel.

This report details the manufacture and testing of a red GaAs LED.

## 2 Fabrication

### 2.1 Cleanrooms

Fabrication of electronic devices takes place in a cleanroom. Cleanrooms are controlled environments where atmospheric conditions are controlled. The class of a cleanroom specifies the number of particles of various sizes for a give volume of air. Guaranteeing the number and size of contaminating particles in a fabrication process gives a reasonable approximation as to the feasibility and the probability of success. As devices become smaller, the need for better cleanrooms increases since smaller particles will have a greater effect on the performance and yield of the devices.

### 2.2 Cleans

Prior to spinning the photoresist for both the p-contact and the mesa etch, the substrates were cleaned to ensure that there was no contamination on the surface and to ensure that the photoresist was deposited correctly.

The cleaning process comprised of 3 minutes in an ultrasonic bath each for OptiClear, acetone and isopropanol (IPA) to remove any particles or organic compounds on the substrate surface. Special attention was given when transferring the substrate from the acetone to the IPA so that the acetone did not dry out and leave a residue. The substrate was then rinsed briefly in RO water before being dried thoroughly by the N2 gun. Lastly the substrate was ashed in an oxygen plasma for 3 minutes at 150W.

### 2.3 Photolithography

For the photolithography steps, the substrate was placed on a suitably sized vacuum chuck in a resist spinner. The vacuum was checked before spinning to ensure the substrate did not come off at high spin speeds. The resist used was Microposit S1818 which was spun at 4000rpm for 30 seconds. According to the S1800 series datasheet [1], this would result in the desired resist thickness of  $1.8\mu\text{m}$ . The S1818 was filtered as it was deposited and it was made sure the the majority of the substrate was covered prior to spinning

After spinning the back of the sample was cleaned with cotton bud soaked with acetone. This removed any unwanted photoresist and stopped the back of the sample contaminating or sticking to the hotplate.

After spinning the substrate was baked on a hotplate at  $115^{\circ}\text{C}$  for 120 seconds. This hardened the photoresist enough so that it would not stick to the photomask or that the resist structure would not collapse and distort after developing.

The SUSS MicroTec MJB4 mask aligner was used to align the masks on the substrate with a hard contact which results in more precise developing when compared to a soft contact

The resist was then developed in a 1:1  $\text{H}_2\text{O}$ :Microposit developer concentrate for 75 seconds. After being rinsed in RO water and dried with the N2 gun, the substrate was again ashed in an oxygen plasma for 3 minutes at 150W to remove any residual resist.

## 2.4 Etching

Before etching, the depth of the resist was found to be  $2022\text{nm}$  by the stylus profiler. The exposed areas of the substrate were wet etched for 60 seconds using a  $\text{H}_2\text{SO}_4:\text{H}_2\text{O}_2:\text{H}_2\text{O}$  1:8:40 solution. The resist depth was measured again and found to be  $2273\text{nm}$  giving an etch depth of  $251\text{nm}$ . Since the thickness of the p+ GaAs contact layer is  $150\text{nm}$ , the etch will have gone  $101\text{nm}$  into the p-InGaAsP layer assuming the layer thicknesses are exact.

Another etching process is dry etching where the etchant is either a gas or plasma. Dry etching can have a slower etch rate and poorer selectivity than wet etching.

## 2.5 Metallisation

After developing the photoresist, the p-contact was metalised by evaporation deposition with Ti/Au  $20/200\text{nm}$ . The back contact was then metalised by the same process with Ni/Au/Ge/Ni/Au  $5/88/12/12/35\text{nm}$ .

After deposition, the metal was annealed by rapid thermal anneal at  $400^\circ\text{C}$  for 30 seconds. Annealing may be done for many reasons. It can reduce the resistance of the metal-semiconductor junction by reducing the trap density. The effect of this was not directly measured as the I-V response of contacts was not measured prior to annealing.

## 2.6 Lift-Off

Once the resist has been exposed and developed and the metallisation steps have been completed, the remaining resist can be stripped leaving the desired metal patterns. The metal on the top of the resist will be removed alongside the resist, and the metal in contact with the substrate will remain. Figure 1 demonstrates this graphically.

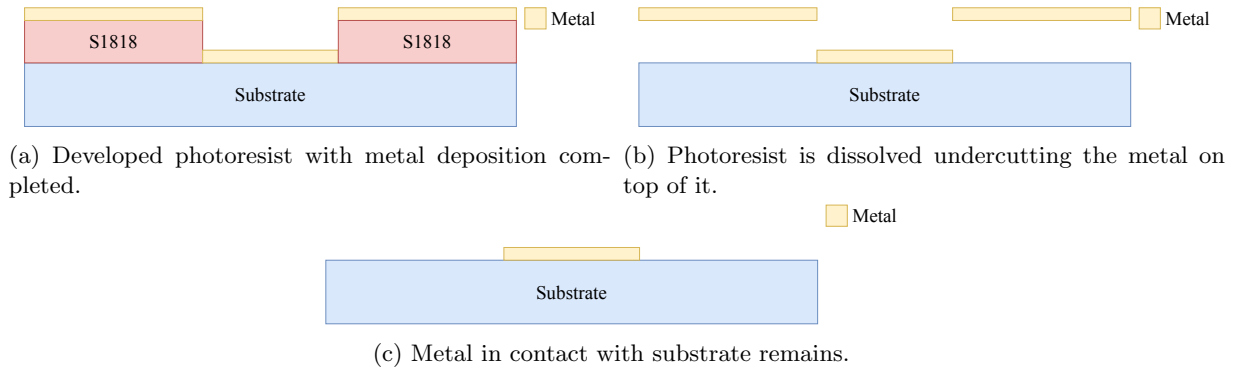


Figure 1: Graphical representation of the lift-off process

For this process, the substrate was placed in a beaker of acetone in a  $50^\circ\text{C}$  bath for a few hours to dissolve the undeveloped resist. It was then cleaned in IPA to remove any acetone residue.

Either electron-beam lithography or a negative photoresist could also have been used to achieve the same metal pattern. E-beam would likely be unsuitable since the minimum feature size doesn't warrant it and if a negative photoresist process were to be used the photomask would need to be inverted.

## 3 Test

### 3.1 Apparatus

Figure 2 shows a schematic of the apparatus used to test the LED. This consisted of a power meter, a camera, and a spectrum analyser. The measured power on the power meter will not be absolute but rather as an indication relative to other measurements on the same apparatus. This is true for two reasons. The light goes through beam splitters before being measured. Also, the light from the LED emits light in all directions so only a fraction of the light pass through the apparatus in the first place.

Three beam splitters were used. The first was to allow a white LED to illuminate the stage. The second split the beam between the camera and the testing equipment. The last split the beam between the spectrum analyser and the power meter.

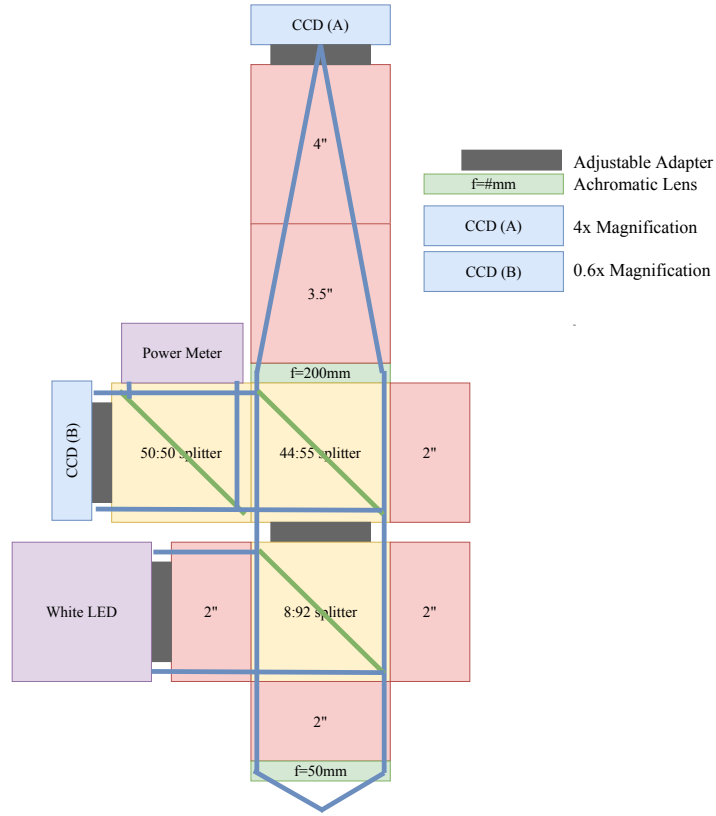


Figure 2: Schematic of the Test Apparatus. The device to be tested is placed at the focal point below the lens with a focal length of  $50\text{mm}$

The optical power measured by the power meter should ideally be 20.7% of the power incident on the first lens.

### 3.2 I-V Characteristics

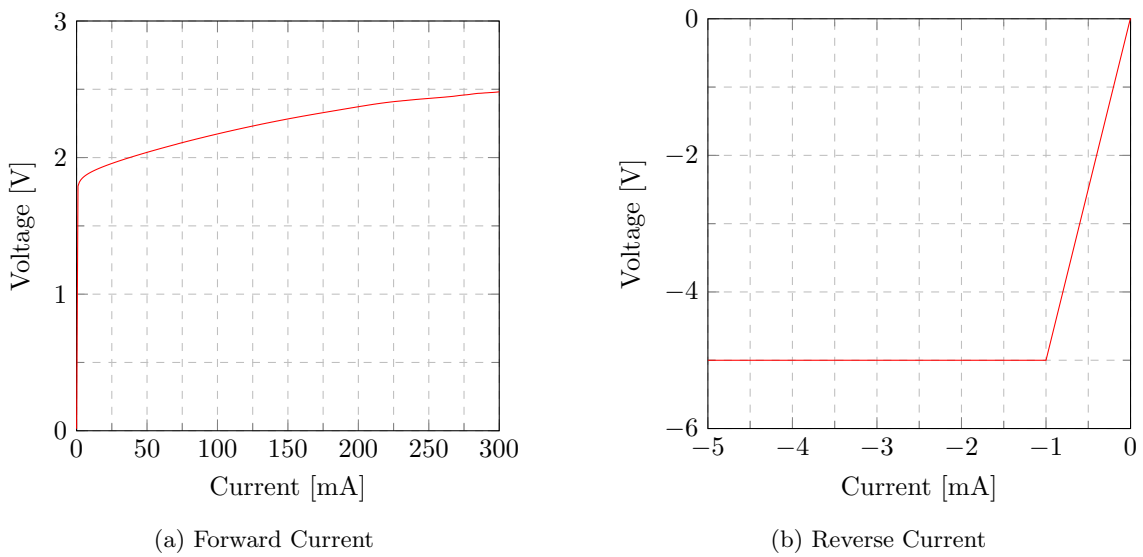


Figure 3: IV characteristics for forward and reverse currents on the LED.

Figure 3 shows the forward and reverse current plots for this LED. The forward voltage turns on at  $1.8\text{V}$  and increases to  $2.5\text{V}$  at  $300\text{mA}$ . The reverse voltage does not show a great deal. The voltage was

limited to a range of  $-5V$  to  $5V$  and the first data point at  $-1mA$  required more than  $-5V$ . As such, it shows a  $-5V$  for all measured currents.

### 3.3 LI Characteristics

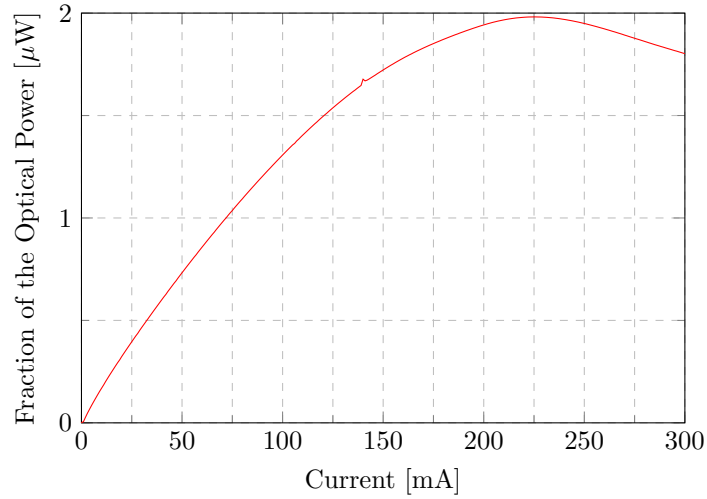


Figure 4: Fraction of the optical power plotted against the forward current of the LED showing the optical power peak at  $220mA$

The optical power was measured against current from  $0mA$  to  $300mA$ . As described in section 3.1, the power measured is not the total output power but a fraction. The results measurements are plotted in 4. This figure shows the optical power increase from  $0mA$  to  $220mA$  before decreasing again as the current increases to  $300mA$ . The peak power is not of any particular interest since it is not absolute but the current at which it occurs,  $220mA$ , is.

### 3.4 Spectral Characteristics

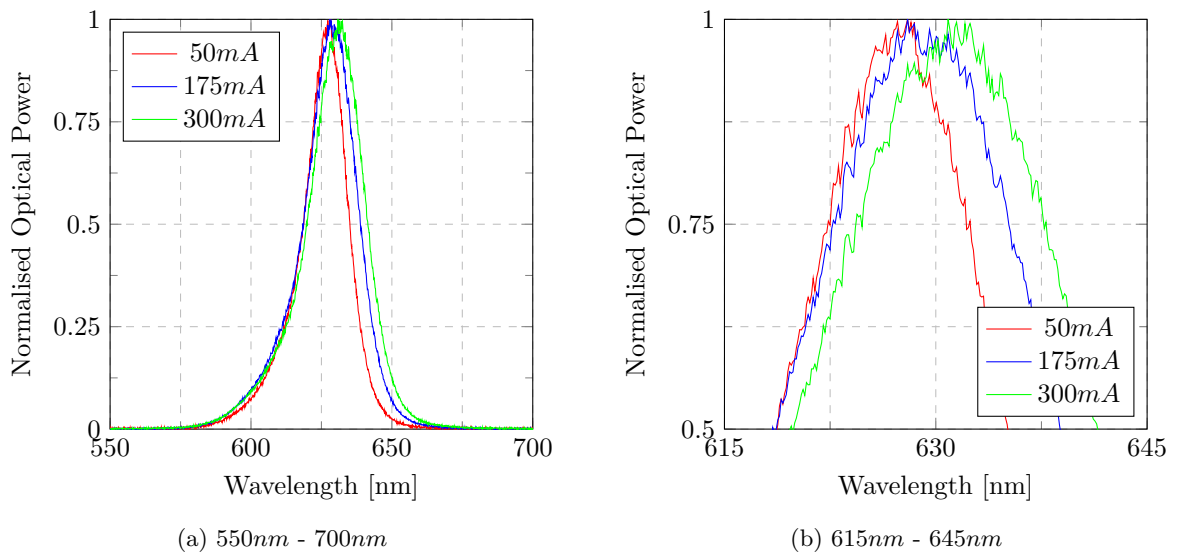


Figure 5: Normalised spectral characteristics for currents of  $50mA$ ,  $175mA$ , and  $300mA$

The emission spectra of the LED are plotted in figure 5. The spectrum was measured at  $50mA$ ,  $175mA$  and  $300mA$ . All plots are normalised to better understand the differences in spectrum. The peak optical power is around a wavelength of  $630nm$ . The exact peak is difficult to determine due to the

noise on the measured signal, see figure 5b, but can be estimated to be approximately  $627nm$ ,  $629nm$ , and  $632nm$  for  $50mA$ ,  $175mA$  and  $300mA$  respectively. Even without a precise value, it is clear that there is a trend that the peak wavelength increases with the current. It is also noticeable that the lower the current, the tighter the wavelength is around its peak.

### 3.5 Contact Resistance

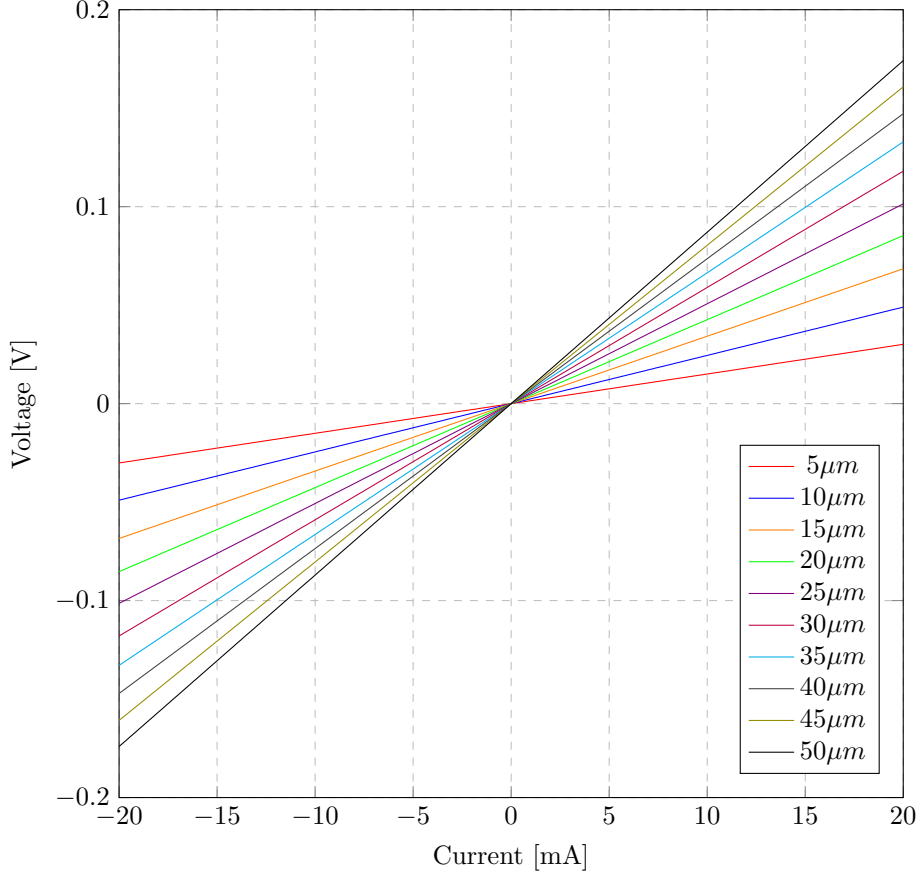


Figure 6: I-V Plot for CTLM Gaps from 5 to  $50\mu m$

Figure 6 shows the I-V plot for all gap size measurements from the circular transfer length method (CTLM). The CTLMs had a radius of  $200\mu m$  and gap sizes from 5 to  $50\mu m$  in steps of  $5\mu m$ . The plots for all gap sizes are close to linear implying that the contacts have an ohmic response.

The average resistance for each gap was found and plotted against the gap sizes, see figure 7. The true gap sizes were not measured and are assumed to be exactly as designed. Due to the nature of CTLMs, the radii of the two contacts cannot be equal. It is therefore necessary to include a correction factor which is found using equation 1

$$C = \frac{1}{R_1} \ln\left(\frac{R_1 + S}{R_1}\right) \quad (1)$$

When the line of best fit for the corrected resistance values, shown in red, on figure 7 are extrapolated it is found that the resistance values when the gap size is  $0\mu m$  the resistance is  $0.659\Omega$ . This is equivalent to  $2R_c$ .

## 4 Commentary

If the fabrication process were to be repeated in future, the etch time would be reduced since it etched 67% deeper than intended. The time would initially be halved then the depth measured before continuing the

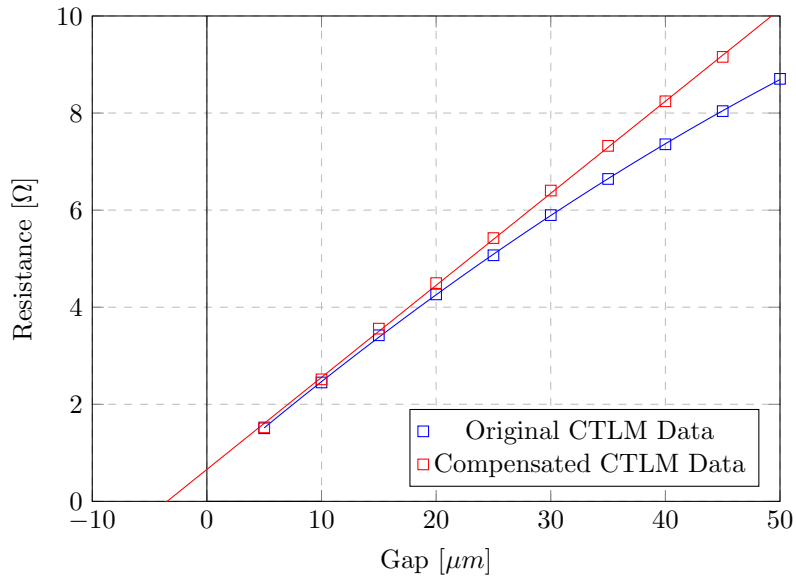


Figure 7: Plot of resistance against CTLM gap size with the as measured data in blue and the data with the correction factor shown in equation 1 applied shown in red. From the graph  $2L_T = 3.473\mu m$  and  $2R_c = 0.659\Omega$

etching in 5 second periods. If the photomasks were to be redesigned at any point, careful consideration should be given to the alignment markers since they did not align.

If the scribe and break process was moved to the end, there it would be possible to use the CTLM to characterise a much larger number of LEDs with the same amount of measurements. Approximately 25% of the current design is given over to testing whereas the same area could be used on a much larger wafer and drastically increase the yield.

The larger mesa diameters used by other students resulted in both more optically powerful LEDs and a larger current draw.

## References

- [1] Shipley microposit s1800 series photo resists. [Online]. Available: [https://amolf.nl/wp-content/uploads/2016/09/datasheets\\_S1800.pdf](https://amolf.nl/wp-content/uploads/2016/09/datasheets_S1800.pdf)